



# HHS Public Access

Author manuscript

*Br J Pharm Res.* Author manuscript; available in PMC 2016 June 13.

Published in final edited form as:

*Br J Pharm Res.* 2015 ; 7(6): 457–476. doi:10.9734/BJPR/2015/19156.

## Diverse Data Sets Can Yield Reliable Information through Mechanistic Modeling: Salicylic Acid Clearance

G. M. Raymond<sup>1</sup> and J. B. Bassingthwaite<sup>1,\*</sup>

<sup>1</sup>Department of Bioengineering, University of Washington, Seattle, USA

### Abstract

This is a practical example of a powerful research strategy: putting together data from studies covering a diversity of conditions can yield a scientifically sound grasp of the phenomenon when the individual observations failed to provide definitive understanding. The rationale is that defining a realistic, quantitative, explanatory hypothesis for the whole set of studies, brings about a “consilience” of the often competing hypotheses considered for individual data sets. An internally consistent conjecture linking multiple data sets simultaneously provides stronger evidence on the characteristics of a system than does analysis of individual data sets limited to narrow ranges of conditions. Our example examines three very different data sets on the clearance of salicylic acid from humans: a high concentration set from aspirin overdoses; a set with medium concentrations from a research study on the influences of the route of administration and of sex on the clearance kinetics, and a set on low dose aspirin for cardiovascular health. Three models were tested: (1) a first order reaction, (2) a Michaelis-Menten (M-M) approach, and (3) an enzyme kinetic model with forward and backward reactions. The reaction rates found from model 1 were distinctly different for the three data sets, having no commonality. The M-M model 2 fitted each of the three data sets but gave a reliable estimates of the Michaelis constant only for the medium level data ( $K_m = 24 \pm 5.4$  mg/L); analyzing the three data sets together with model 2 gave  $K_m = 18 \pm 2.6$  mg/L. (Estimating parameters using larger numbers of data points in an optimization increases the degrees of freedom, constraining the range of the estimates). Using the enzyme kinetic model (3) increased the number of free parameters but nevertheless improved the goodness of fit to the combined data sets, giving tighter constraints, and a lower estimated  $K_m = 14.6 \pm 2.9$  mg/L, demonstrating that fitting diverse data sets with a single model improves confidence in the results. This modeling effort is also an example of reproducible science available at <http://www.physiome.org/jsim/models/webmodel/NSR/SalicylicAcidClearance>

---

This is an Open Access article distributed under the terms of the Creative Commons Attribution License (<http://creativecommons.org/licenses/by/4.0>), which permits unrestricted use, distribution, and reproduction in any medium, provided the original work is properly cited.

\*Corresponding author: [jbb2@u.washington.edu](mailto:jbb2@u.washington.edu).

#### Authors' contributions

This work was carried out in collaboration between the two authors, who shared the effort in each of the stages. Both authors read and approved the final manuscript.

#### COMPETING INTERESTS

Authors have declared that no competing interests exist.

## Keywords

Briggs-Haldane; clearance; enzyme; half-life; JSim; Michaelis-Menten; model; reproducible; salicylic acid; salicylurate; CoA; aspirin; multilevel systems; confidence ranges

---

## 1. INTRODUCTION

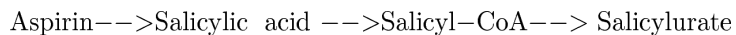
The purpose of this presentation is to demonstrate that useful information can be gleaned from the literature by putting together disparate data sets that can be integrated to yield a quantitative interpretation that could not be obtained from any of the individual data sets. We start with three clinical data sets on the clearance of aspirin from the blood. These were studies on humans, one in the range of normal therapy (10–70 mg/L, plasma levels; dose 1000 mg), one in people poisoned by overdosing (> 250 mg/L, high doses), and one on the kinetics of disappearance of the 80 mg antiplatelet dose (< 6 mg/L). The principle on which this essay is based is that we can gain mechanistic insight by analyzing the three data sets together but not from any of the individual data sets. Further, despite the fact that we use only crude, accumulated average values from different populations of patients and experimental subjects, and use no information on actual biochemical kinetics, we can present an analysis of predictive value that may be used to understand the observations and to guide therapy.

In this study, we examine data on aspirin that were gathered in three unrelated clearance studies. Thinking pharmacokinetically, one wants to interpret data in parametric terms (rate constants, enzyme affinities, membrane permeabilities, etc.) that represent the processes and provide insight into mechanism. We take advantage of the wide ranges of concentrations observed, trying to identify rate constants and affinities that should be common to the three diverse data sets.

Aspirin, acetyl salicylic acid, is rapidly hydrolyzed to acetate and salicylate. Salicylate is the effective therapeutic agent at 30 to 80 mg/L. The drug's efficacy is limited by its degradation. Mitochondrial enzymes in liver and kidney degrade salicylate to an inert product, salicylurate, that is, like salicylate itself, excreted in the urine. Binding to plasma proteins retards renal clearance of salicylate, prolonging its retention, so that most of the renal excretion is as the salicylurate. Concentrations ten times therapeutic levels are toxic, causing acidosis, and sometimes death. The LD50 (lethal dose for 50% of subjects) is about 200 mg/kg in rats and mice and probably higher in humans, i.e. of the order of more than 10 grams for a 50 kg person. Historically, fevers, pains, and inflammation were treated with preparations from willow bark from Greek times. Salicylate was explicitly identified by Stone [1]. Aspirin, acetyl-salicylate, was synthesized and marketed by Bayer in 1897, and continues to be in wide use with few problems.

## 2. OVERVIEW OF THE KINETICS

The substrate to product reaction sequence,  $S \rightarrow P$ , is:



The hydrolysis to salicylic acid is so fast that it can be considered instantaneous. The rate-limiting step in degradation is the conversion of salicylic acid to salicyl-CoA catalyzed by medium chain acyl-Coenzyme A synthase, and the final step is the conversion of salicyl-CoA to salicylurate, catalyzed by glycine-N-acyltransferase [2]. The conversion to salicylurate is a key step toward renal clearance, accounting for 50% [3,4] to 85% [5] of ingested salicylate. Only about 10% is urinary salicylate [6]. Presumably renal clearance by passive filtration across the glomerular membrane is zero for salicylate bound to plasma albumin, and may be slower for the ionized fraction of salicylate because of the charge. In any case the clearance basically follows the conversion to salicylurate.

We define a minimal model in which the whole body is considered as a mixing chamber into which the salicylate is absorbed, and within which an enzyme converts salicylate to salicylurate. Salicylurate is assumed to be the only product, and the only solute cleared by the kidney, ignoring the salicylate 10% mentioned just above. The converting enzymes are in mitochondria in the liver and kidney, not free in the circulation: the kinetic simplicity of the model makes sense only if the whole body mixing and the transport from blood to mitochondria are both fast compared to the conversion steps and the renal clearance.

Three models to describe and “explain” the clearance of the salicylate will be explored: (1) the first tests the concept that first order kinetics dominate the system, as if the clearance were controlled by a single exponential washout process, a totally inadequate model; (2) the second model asks if a Michaelis-Menten enzymatic reaction model can define the kinetics; (3) the third test is a more fully developed enzyme kinetic model with reversible reactions. Each model is tested against the three data sets individually and then together, asking whether or not the data from three different sets of subjects at three very different levels of dosage can be “explained” in terms of *one* structurally and parametrically self-consistent model describing the processes governing the clearance. We say “explain” in quotes since all models are incomplete and inexact.

### 3. THE DATA AND THE SOURCES

The data sets are group-averaged observations on plasma salicylate concentrations as a function of time over most of a day after ingestion of aspirin. The data were published in three unrelated studies, each of which covered a different range of concentrations (Fig. 1).

The data (Fig. 1 left) for low dose aspirin ingestion [7] are the averaged plasma concentrations from ten healthy male volunteers who ingested an 81 mg tablet of aspirin. The last seven points were digitized from the authors' figure (their Fig. 1, right panel, dose period 1, open squares). “All aspects of the study were conducted in accordance with regulations of the United States Food and Drug Administration (FDA), in particular those regarding informed consent and approval by a qualified Institutional Review Board”.

The data (Fig. 1 middle) for mid dose aspirin ingestion [8] are the averaged plasma concentrations from 9 female and 9 male healthy volunteers, who ingested 1000 mg of lysine acetyl salicylate. The last eleven points were digitized from authors' Fig. 3, the solid triangles. "Each subject gave informed written consent to participate in the study and the study received the approval of an Ethics Committee".

The data (Fig. 1, right) for the high dose aspirin ingestion [9] are the averaged plasma concentrations from 16 patients being treated for mild poisoning, salicylism, (plasma salicylate concentrations 250–400 mg/L). The last nine points were digitized from authors' figure (their Fig. 1, open circles). In these aspirin overdose cases, the authors were attempting to discern best treatment methods. The research was performed at the Regional Poisoning Treatment Centre and University Department of Therapeutics and Clinical Pharmacology, Royal Infirmary, Edinburgh EH3 9YW. "All patients were conscious and recovered uneventfully".

## 4. METHODS OF ANALYSIS

We used a general-purpose simulation system, JSim [10], designed for data analysis, displaying results and storing them as Reproducible Exchange Packages (REP). JSim code for the three models is written in MML, Mathematical Modeling Language: the equations have the same form as one would write them on paper, with the exception that the derivative  $dS/dt$  is written  $S:t$ . Routines for solving ordinary differential equations (ODEs), partial differential equations (PDEs) and differential algebraic equations, are built into JSim and selected by the user. JSim provides 8 methods for solving ODEs, three for PDEs. Comparing different methods is a key step in code *verification*, a part of demonstrating its correctness. Eight optimizers are available for automated fitting of model solutions to data; switching from one method to another helps to determine the uniqueness of the fit. At the point of best fit both an analytical method (covariance matrix) and MonteCarlo (randomized) method are used for estimating confidence limits, and projecting uncertainty quantification. The REP provides storage of all data, figures and parameter files and retention of all the models developed for a project, in a form reproducible under Linux, MacOS X or Windows. Model code is in the APPENDICES. The models used in the analysis are installed at <http://www.physiome.org> and can be run over the web. They are open source and open operation, and may be downloaded from there, as can JSim itself. All data files, models, initial conditions, parameters, and resulting figures for this report are completely described in the REP file at <http://www.physiome.org/jsim/models/webmodel/NSR/SalicylicAcidClearance>

### 4.1 Model 1: A Descriptive First-order Washout Model

The single exponential decay or first-order process is based on the expectation that there is a single means of clearance from the body and that it is passive, whereby a constant fraction of the concentration is removed per unit time, independent of the concentration. Assuming that mixing within the body is fast compared with the rate of removal, then, using  $S$  for salicylate concentration mg/L, and  $k$  as the fraction removed per minute, the removal flux is  $k$  times  $S$ . For a given initial concentration  $S(t=0) = S_0$ , the governing ordinary differential equation (ODE) is

$$dS(t)/dt = -k \cdot S(t). \quad (1)$$

The solution to this ODE is

$$S(t) = S_0 \cdot \exp(-k \cdot t) \quad (2)$$

A semilog plot would give a straight line, a constant fraction lost per unit time. When half of the substance is gone, the solution becomes

$$S_0/2 = S_0 \cdot \exp(-k \cdot t_{\text{half}}). \quad (3)$$

Defining the half-life as

$$t_{\text{half}} = \log_e(2)/k \quad (4)$$

allows one to rewrite Eq. 1 as

$$dS(t)/dt = -(\log_e(2)/t_{\text{half}}) \cdot S(t). \quad (5)$$

The descriptive parameters,  $k$  and  $S_0$ , for the model were adjusted to fit the data by minimizing the weighted sums of square of the distances between the data points and the model solutions, the Sum of Squares of Weighted Residuals, SSWR. This can be done either manually or by automated optimization. The model code is in Appendix 1. The “import nsrunit; unit conversion on;” requests the parser (a precompiler phase) to check the equations, and any exponents or transcendental functions like sine, for unit balance [11]; the parser also inserts reconciling conversion factors, e.g. 60 sec/min, when analogous units have been used.

This is automatic, and is the first step in verifying that the model code is computing correctly, a part of JSim’s design to support the project from experiment through the steps of a VVUQ process, model development, *Verification* that the code computes correctly, *Validation* that the model can be fitted to experimental data, and *Uncertainty Quantification* in parameter identification, in estimation of confidence limits from the sensitivity functions or from Monte Carlo, and in making predictions.

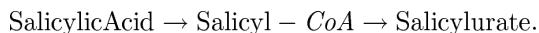
The Model 1 parameters for initial concentrations (LS0, MS0, and HS0) and the respective rate constants, Lk, Mk, and Hk (or alternatively the half lives), may be manually adjusted to fit the data. The same process can be automated using the “Optimization” Graphical User Interface (GUI). The optimization GUI is used to automate the fitting to each data set individually to estimate the decay rate and the initial concentrations; these are reported in Table 1, along with the standard deviations estimated from the covariance matrix.

As a test to see if clearance was by a single passive first order process we optimized the model solutions to use a single decay rate to best fit the three data sets simultaneously. This idea was disproved; a single decay slope could fit only one of them reasonably well at a time. Their initial values were strikingly different, so the only situation that would give similar decay rates for the three sets of data would be if their clearances mechanisms were the same, e.g. renal clearance by glomerular filtration. This was clearly not the case, so we rejected the hypothesis of a common factor being renal passive clearance.

What we learn from this model is that decay rates are slower at high concentrations (Table 1). Raising the initial concentrations by two orders of magnitude increases the half-lives by over tenfold. The time courses of the high dose concentrations and the upper range of the mid dose concentrations are approximately linear, suggesting that a zero-order process ( $S$  is removed at a constant rate) might be a better model. The last points of the mid dose and all the low dose concentration-time curves are nevertheless close to an exponential decay. Putting these observations together suggests that another model, a saturable enzyme model might be better; more explicitly, a saturable enzyme model with a  $K_m$  somewhere between the low dose concentrations and the medium dose concentrations would make sense.

#### 4.2 Model 2: The Michaelis-Menten Model for Enzymatic Reaction

The reaction sequence  $S \rightarrow P$  for salicylurate formulation is



The Michaelis-Menten [12] model assumes that there is no reverse flux from salicylurate, the product  $P$ , back to substrate  $S$ . Most of the clearance of  $S$  follows conversion of  $S$  to the metabolite,  $P$ , which is cleared by the kidney.

Using a single mechanistic model to fit the three data sets simultaneously should be more powerful than obtaining three independent half-life estimates, because of increasing the degrees of freedom by virtue of the constraints: more data means larger  $n$ , and the fewer parameters, one  $K_m$  and one  $V_{max}$  instead of 3 decay rates, means a tighter focus, fewer parameters per data point. Using all the data simultaneously focuses the analysis on the characteristics of an explanatory mechanism, enzymatic degradation (Fig. 2).

$S$  is the substrate, salicylic acid,  $E$  is the enzyme, medium chain acyl-Coenzyme A synthetase, and  $SE$  is the enzyme-substrate complex, and  $P$  is still the product, salicylurate. Our assumption in this formulation is that  $SE$ , the enzyme-substrate complex, and  $PE$ , the enzyme-product complex are instantaneously interconvertible and can be regarded as the same species. The four reactions are considered to be reversible. This results in a system of four ODEs with initial conditions (Eqs. 6, 7, 8, 9, and 10) using mass balance equations

$$dS/dt = -k_{on1} \cdot S \cdot E + k_{off1} \cdot SE \quad (6)$$

$$dSE/dt = k_{on1} \cdot S \cdot E - (k_{off1} + k_{off2}) \cdot SE \quad (7)$$

Conservation of enzyme mass allows an algebraic expression for E instead of an ODE:

$$E = E_{TOT} - SE. \quad (8)$$

Salicylurate, P, is formed in the reaction, but is also removed by other processes, potentially by the reverse reaction with rate kon2 for backward binding to the same enzyme, or by conversion to other substances, represented by the consumption reaction at rate G:

$$dP/dt = -k_{on2} \cdot P \cdot E + k_{off2} \cdot SE - G \cdot P. \quad (9)$$

For the most part, we will set G to zero and ignore the effect of the removal of P. The initial conditions are given as

$$S(t=0) = S_0; SE(t=0) = 0; E(t=0) = E_{TOT}; P(t=0) = 0; \quad (10)$$

The Michaelis-Menten (M-M) equation is identical to the Briggs-Haldane (B-H) equation [13], but they are derived via different assumptions from Eqs 6 and 7. B-H is based on the intermediate complex, SE, being in quasi-steady state, specifically  $dSE/dt$  is small compared to the rate of change of S and P. M-M is based on the substrate, S, and the complex, SE, being in rapid equilibrium with high on- and off-rates so that the ratio E/ES is continuously defined in accord with the dissociation constant  $K_S$ :

$$K_S = k_{off1}/k_{on1} = E \cdot S/SE. \quad (11)$$

The parameter kon2 for the reversal of the product formation is assumed to be zero for the M-M model, but for the data shown is probably not true. The final equation in both cases, which we will call the Briggs-Haldane / Michaelis-Menten model (B-H/M-M), is

$$dS/dt = -V_{max} \cdot S/(K_m + S), \quad (12)$$

where S is the concentration or activity of the substrate,  $V_{max}$ , the maximum velocity of the reaction is given by

$$V_{max} = k_{off2} \cdot E_{TOT}. \quad (13)$$

The substrate concentration at which the reaction velocity is half of  $V_{max}$  occurs when the enzyme is half occupied, i.e.  $[ES]/[E_{TOT}] = 0.5$ , and accounts for the conversion of ES forward to P and backward to S. This defines  $K_m$  from Eq. 13 as

$$K_m = (k_{off1} + k_{off2})/k_{on1} \text{ or } K_m = K_s + k_{off2}/k_{on1} \quad (14)$$

illustrating that when the forward, product-forming reaction is slow compare to the binding on- and off-rates that  $K_m$  is only slightly greater than  $K_s$ . When the concentration,  $S$ , is small compared to  $K_m$  (as in the low dose case), the ODE for  $S$  approaches

$$dS/dt \approx -(V_{max}/K_m) \cdot S, \quad (15)$$

which is a first order process with the solution defining that for this situation  $V_{max} / K_m$  equals the  $k$  of Model 1 for the first order reaction process. When the concentration  $S$  is large compared to  $K_m$ , then  $S / (S + K_m)$  approaches 1, and the ODE for  $S$ , Eq. 16, approaches

$$dS/dt \approx -V_{max}. \quad (16)$$

This is a zero order process with solution  $S(t) = S_0 - V_{max} \cdot t$ . Thus the B-H/M-M model can be zero-order at high concentrations and first order at low.

The M-M code in MML is in Appendix 2. For starting values for data fitting, we estimated  $V_{max}$  using the first and last points of the high dose curve [9] to approximate Eq. 17 as

$$V_{max} \approx -dS/dt \approx -\Delta SA/\Delta t \approx -(341\text{mg/L} - 225\text{mg/L})/(.95\text{hour} - 15.94\text{hour}) \approx 7.7\text{mg}/(\text{L}\cdot\text{hour}). \quad (17)$$

This is about 2% per hour in these aspirin-poisoned patients. From the low dose data [7] we estimate a rate constant using

$$-d\log(S/S_0)/dt = V_{max}/K_m \approx -\partial\log(S/S_0)/\partial t = -\Delta \log S/\Delta t. \quad (18)$$

$V_{max} / K_m = \log((2.483 \text{ mg/L})/(0.184 \text{ mg/L})) / ((12.032 \text{ hour}) - 1.888 \text{ hour}) = 0.257 \text{ hour}^{-1}$ , and using the estimated value for  $V_{max}$ , we obtain a starting estimate for  $K_m$ , namely,  $K_m = V_{max}/(0.257 \text{ hour}^{-1}) = (7.7 \text{ mg}/(\text{L}\cdot\text{hour})) / (0.257 \text{ hour}^{-1}) = 30.0 \text{ mg/L}$ . This is higher than the estimate of  $K_m$ , 16.5 mg/L, from Ho et al. [14].

For automated optimization we set the point weights to 1. For fitting the three data curves simultaneously we assigned *curve weights* that were high for the low dose data, and low for



the high dose data, as stated above, so that they have similar total weight in the weighted sum of squares (Table 2, next to bottom row). The sum of squares of the differences between data and model solution for the individual data set are in the bottom row in Table 2. (A sum of the individual differences divided by the individual model point values, divided by Npoints for the individual data set, gives the fractional residual error; this is useful for comparisons amongst the individual data set fits.) The fit to the three data curves using single common values for  $V_{\max}$  and  $K_m$  is shown in Fig. 3.

In Fig. 4 we plot the flux, the rate of disappearance of S (enzymatic degradation) or  $-dS/dt$  calculated from the model solutions versus the observed concentrations, the data. The intersection of this curve with  $V_{\max}/2$  gives  $K_m$  on the abscissa. Fluxes at the high concentrations are close to the upper limit at  $V_{\max}$ .

What did we learn from the irreversible M-M model? Firstly, the parameter values of this model were not well defined by fitting the individual data curves: at the low and the high concentrations the variances were worse than those for the first order washout model 1. However, when the *three* data sets were fitted with *one* set of parameters the estimates were well defined, with much smaller coefficients of variation, SD/Mean, for both the low and high concentration data. This makes for a good generality: in order to estimate  $K_m$  the experiment must provide data over a *wide range* and the range must encompass the  $K_m$ . On comparing the estimates for the mid range data alone with those from the values for the three sets together, they are not statistically significantly different. The fluxes are linearly related to  $S/(S+K_m)$ ; their range is greatest for the mid level data, the triangles in Fig. 4, where the ratio of flux to concentration changes steeply in the neighborhood of the  $K_m$ . At levels below  $K_m/10$  and above levels of  $10 K_m$ , the slopes of flux versus concentration are shallow, and therefore nearly impossible to use to estimate  $K_m$  accurately. Even  $V_{\max}$  is poorly estimated from the high concentration data: when the enzyme is nearly saturated, with zero order kinetics, all one knows from the high dose data alone is that the concentrations are many times the  $K_m$ .

### 4.3 Model 3: Enzyme Kinetic Model with Binding Rate Coefficients and Reversibility

The third model incorporates reactions implied in Fig. 2 and defined in Eqs 7 to 10. Since all chemical reactions are in principle reversible, the model has a reverse flux  $P \rightarrow S$ , and thus allows comparing the results with those from the irreversible B-H/M-M formulation. A preliminary treatment was presented in [15]. We lack early samples that might have provided information on the rapidity of binding, so in accord with expected small solute binding to proteins we assume that  $k_{on1}$  is high, e.g. we use 3 L/(mg\*sec), of the same order as fatty acids to albumin. The rate of product formation is governed by  $K_S$ ,  $k_{off2}$ , and  $K_m$ , the combination of the first two giving us  $K_m$  (Eq.15). The maximum forward velocity of the reaction is  $V_{\max}$ , which is the product  $E_{TOT}k_{off2}$ . From the experience with model 2 (M-M) we know that the strongest parameter estimation method is to use the three experimental data sets simultaneously, together they cover three orders of magnitude of concentrations. Not knowing the affinity  $K_P$  for the product, but given that reactions are reversible, the long tail of concentrations for low dose data suggest that this reaction is demonstrating its reversibility. Since P was not measured one cannot hope to obtain a unique estimate of  $K_P$ ,

even though the reverse flux must occur at all three concentration levels. Analogous to  $K_S$  in Eq. 12, the dissociation constant  $K_P$  defines the equilibrium condition for  $P$ ,  $E$ , and  $EP$  such that:

$$K_P = k_{\text{off}2} / k_{\text{on}2} = E \cdot P / EP \quad (19)$$

where  $EP$  is considered identical to  $ES$  through their instantaneous interconvertibility. The model 3 code to optimize to fit the three data sets simultaneously with one set of parameters as in Appendix 3.

Eqs. 7 to 10 concern the conversion of salicylic acid to salicylurate. We guesstimate  $E_{TOT}$ , the concentration of medium chain acyl-CoA synthetase, to be  $1.5 \times 10^{-4}$  mg/L, taken from the geometric mean of estimates for the human acylcoenzyme A synthetase ACSM2B, mitochondrial (ACSM2B) ELISA Kit ([http://www.mybiosource.com/datasheet.php?products\\_id=911502](http://www.mybiosource.com/datasheet.php?products_id=911502)). We set  $k_{\text{on}1}$  to be  $\sim 3/\text{sec}$  or  $\sim 10800/\text{hour}$ , then optimized to estimate the remaining parameters in three different situations: (A) fitting the individual data sets, (B) fitting the three data sets simultaneously to estimate for  $K_S$ ,  $K_P$ , and  $k_{\text{off}2}$  and the three “initial” concentrations, and (C) fixing the three initial concentrations to the values found in B and optimizing only the kinetic parameters,  $K_S$ ,  $K_P$ , and  $k_{\text{off}2}$ . From the optimized parameters we *calculated* the effective Michaelis-Menten parameters,  $K_m$  and  $V_{\text{max}}$ , reported in Table 3 in the fourth and third rows from the bottom. The estimate of  $K_m$  is slightly lower than those reported by Levy [4]. The derived estimates for  $k_{\text{off}1}$ , the rate of complex dissociation to produce free substrate  $S$  from the  $ES$  complex, and  $k_{\text{on}2}$ , the rate of binding of product  $P$  to form  $EP$  (regarded as equilibrated with the  $ES$  form), are reported in the bottom two rows of Table 3. To obtain the estimates of the SD's for the free parameters, 1000 Monte Carlo cases were run for each combination of parameters. To do this we added 1% proportional uniform noise to each data point. Monte Carlo results were rejected when values for  $K_S$ ,  $K_P$ , and  $k_{\text{off}2}$  were over 1000. The fits of the model solutions to the data are in Fig. 5. The low dose data are now better fitted to the tail of the curve, a result of the reverse reaction and the concentrations approaching an equilibrium level between  $S$  and  $P$ .

The decay curve for the low dose (Fig. 5) is no longer a single exponential decay, but is deviating from it by prolonging the tail: small reverse flux from  $P$  to  $S$  keeps the concentration of  $S$  above zero, so this result is substantially different from that in Fig. 3, left. The influence of the concentration of the product  $P$  is small because the enzyme  $E$  has a relatively low affinity for  $P$ , as indicated by the high value for  $K_P$  (Table 3).

With the high dose (Fig. 5, right) the decay is almost linear, showing that the enzyme is nearly saturated and that product is being formed at a rate near  $V_{\text{max}}$ , a zero order process. This is much slower than the rate of decay proportional to concentration observed at low concentrations. The estimated  $V_{\text{max}}$  of  $8.0 \text{ mg}/(\text{L}\cdot\text{hr})$  is almost identical with the crude estimate from the slope in Eq 18.

With the middle dose the fraction of enzyme bound with  $S$  is almost constant until the concentration of  $S$  is less than approximately  $40 \text{ mg}/\text{L}$ . There is a gradual transition from

nearly-saturated conversion initially to closer to first order clearance after 5 hours. The initial rates of removal of  $S$  at high and mid-level concentrations, operating close to  $V_{\max}$ , are described as well by the B-H/M-M model as by this model.

For these fits  $E_{TOT}$  is not optimized since its value is more or less nominal. Its value appears in the calculations always as a part of the product,  $E_{TOT}$  times  $k_{off2}$ . Thus  $E_{TOT}$  and  $k_{off2}$  vary inversely with one another if both are free parameters, and in the correlation matrix would inevitably be highly correlated, in this case around  $r \sim 0.8$ . When covariances are high between pairs of parameters, the estimated standard deviations (SD) will be large. Without data on the concentrations of  $P$ ,  $K_P$  is almost unconstrained. In accord with the M-M concept of rapid equilibration between  $E$ ,  $ES$  and  $S$ ,  $k_{on1}$  was fixed to a moderately high value of 3/sec, which then reduced the SDs of the parameter estimates to about 34% for  $K_S$  and 75% for  $K$ . This illustrates that constraining the degrees of freedom narrows the parameter confidence ranges for the remaining free parameters. When only  $K_S$ ,  $K_P$ , and  $k_{off2}$  were freely adjustable, the SD on  $k_{off2}$  shrunk to  $\sim 3\%$ .

Fig. 6 (top panels) shows the fitting of the concentration-time curves on a semilog plot. On this scale it becomes obvious how much slower is the decay rate for the high concentrations. With the Low dose, the decay is initially almost exponential but the tail begins to level off after 8 hours: the reverse reaction,  $P \rightarrow S$ , provides an explanation for this. The middle dose data are those that give the most definitive information on  $K_S$ : the concentrations pass from above to below  $K_S$ , thus it makes sense that the estimates of  $K_S$  and  $k_{off2}$  from the middle dose data alone (column 3 of Table 3) have much narrower confidence limits than those estimated individually from the low and high doses (columns 2 and 4), and provides an estimate that is not very different from the best estimate provided by analyzing all the data simultaneously.

## 5. ENZYME SATURATION

While it is true that the fastest absolute flux,  $V_{\max}$ , occurs when the enzyme is completely saturated and all of the enzyme molecules are working,  $ES = E_{tot}$ , *the fastest flux per unit substrate concentration* occurs when the substrate has greatest access to the enzyme, namely at low substrate concentrations, when occupancy is lowest. The idea is illustrated in Fig. 6.

With the low dose (left panel) the fraction of enzyme bound,  $SE/E_{TOT}$ , was only 0.3, 30% saturated, at the beginning and fell rapidly to less than 10%. By definition, when the enzyme is unsaturated, the fraction of enzyme molecules available to bind substrate is maximal, resulting in rapid conversion of  $S$  to its metabolite,  $P$ . The fraction of free enzyme  $E/E_{TOT}$  (dotted line) rose toward close to 100% as the reaction depleted  $S$ . The mid dose panel shows that the bound fraction, the substrate-enzyme complex,  $SE/E_{TOT}$  (solid line), was initially high, over 80%, and nearly constant (quasi-steady state): the rate of change of  $SE/E_{TOT}$  was small until the concentration of  $S$  was less than approximately 40 mg/L, after which it diminished increasingly rapidly. In contrast, with the high dose (right panel) the fractional occupancy,  $SE/E_{TOT}$  is over 90%, almost fully saturated, throughout the observation period. In this situation the fraction of the toxic substrate removed per unit time is small, about 2% per hour, and interventional therapy is desired.

## 6. DISCUSSION

The three models used to explain the disappearance of *S*, salicylate, from plasma, where the data came from three separate studies and spanned three orders of magnitude, were: (1) a descriptive first order decay model, chosen since it is the commonest and simplest model used in pharmacokinetic analysis, (2) a Briggs-Haldane/ Michaelis-Menten model, an approximation for an enzymatic reaction, the commonest and most frequently used model in biochemical reactions, though it is thermodynamically undefined. and (3) a thermodynamically based enzyme kinetic model with reversibility, thus fulfilling minimal thermodynamic expectations.

Model 1, first order, could only fit one data set at a time, meaning that the different data sets had unrelated clearance rates. Simultaneous optimization had no role to play since there were no parameters in common. The good individual fits with model 1 cannot be interpreted in terms of one mechanism.

The B-H / M-M formalism, model 2, fitted suitably at all doses, but only for the mid dose data did the fractional enzyme saturation,  $SE/E_{tot}$  shift through 50% and give a measure of the dissociation constant,  $K_S$ . This marks a transition point between a zero order process at the earlier time to a first order process at the later time. For the low dose observations the concentrations were always less than the optimized value for  $K_m$ , but contributed to defining it. But even though the concentrations were low, the decay did not have exactly the expected single exponential form, and instead exhibited a second slower component extending the tail of the curve, a clear deviation. The Briggs-Haldane / Michaelis-Menten model was therefore inadequate even in this region.

The “full” enzyme kinetic model, model 3, even though it does not distinguish  $SE$  from  $PE$ , and assumes that the reversibility in the pocket of the enzyme binding site occurs more or less instantaneously in either direction, properly accounts for the degree of saturation of the enzyme, so the ratio  $SE/E_{tot}$  is correct whether it forms from  $S$  or  $P$ . We could have used Hofmeyr's variant of the M-M model including the reversibility [16]. In a steady state they give the net forward flux,  $V_{fnet}$ , as the difference between the unidirectional forward and the unidirectional backward fluxes:

$$-dS/dt = \frac{(V_{fmax} \cdot S/K_s - V_{rmax} \cdot P/K_p)}{(1 + S/K_s + P/K_p)} \quad (20)$$

where the denominator accounts for the enzyme occupancy by both  $S$  and  $P$ . The number of free parameters, four, is the same, given that we fixed  $k_{on1}$ . In the high dose case particularly the denominator of Eq. 20 is large, as reflected in the slow degradation rate. This model assumes, as do the B-H/M-M models, that  $E_{TOT}$  is small compared to  $S$  and  $P$ . In the particular cases we model, this is also true, but that restriction is not necessarily valid: in any progress curve experiment, as in the low dose case in this study, if product  $P$  were removed continuously the concentration of  $S$  would decrease to zero, violating the assumption that  $E_{TOT}/S$  is small. If  $P$  is not removed, then the system would settle at equilibrium with  $dS/dt$

= 0, and the numerator of Eq 20 would go to ( $V_{fmax} \cdot S / K_s = V_{fmax} \cdot P / K_p$ ), and leads to the equilibrium ratio S/P at

$$\frac{S}{P} = \frac{V_{rmax}}{V_{fmax}} \cdot \frac{K_s}{K_p} = \frac{k_{off1}}{k_{off2}} \cdot \frac{K_s}{K_p} = \frac{k_{off1}^2/k_{on1}}{k_{off2}^2/k_{on2}} \quad (21)$$

Because we have no information on concentrations of P, we have no real information on  $K_p$  or  $k_{on2}$ , but is useful to contemplate what other circumstantial evidence might constrain the estimates. By definition, at equilibrium  $k_{on2} \cdot K_p = k_{off2}$ , so given the estimated values from Table 3 with  $k_{off2} = 14.4/\text{sec}$  and  $K_p = 260 \text{ mg/L}$ , then if we think the low dose data might be reaching a constant S/P equilibrium by 15 hours one could calculate rough estimates of  $k_{on2}$  and conceivably revise the estimates of  $K_p$  from knowledge of the relative renal clearances of P and S.

A reason for emphasizing using the differential equations rather than the algebraic expression in Eq. 21 is that the incorporation of salicylic acid into the salicylate-CoA form is a slow reaction, violating the M-M assumption of fast binding and unbinding. Using the full equations allows this, and the present study shows that the forward reaction is partially limited by both  $k_{on1}$  and  $k_{off2}$ , latter being only 5 times the former. This is important in accounting accurately for rapid changes in concentrations, obviously important in the first moments after injecting or ingesting an actively metabolized substance.

Even while arguing for the “full” model, we recognize many shortcomings our modeling, and in the data. The most obvious and worrisome is the simplification that pretends that the enzyme and the measured concentrations are in the same mixing tank, the circulating blood: the actuality is that the enzyme is really two enzymes [2] and they are not in the blood but in mitochondria of the liver and kidney. The intracellular localization means that a slow  $k_{on1}$  becomes understandable in the light of the time required for convection-permeation-diffusion processes to enter the cells and to permeate the mitochondrial membrane, and for the time to take the same route in reverse for the reaction product, salicylurate to enter the blood and to be cleared into the urine by glomerular filtration. Bloch et al. [17] also model aspirin clearance, reporting similar results with a different modeling system. To assuage our guilt feelings for not accounting for these retarding processes, we developed a crude but more general model that does that. This more complex model (SalicylateBodyMito #377 at [www.physiome.org](http://www.physiome.org)) considers the reactants *S* and *P* and the enzyme *E* to be in the mitochondrial space, so *S* and *P* need to permeate the cell and mitochondrial membranes to exchange with a whole-body-blood-equivalent mixing chamber, in which *S* and *P* are measured, and from which both may be removed by renal clearance. Assuming fairly high permeabilities for *S* and *P*, and analyzing the data as described above, we obtained essentially similar values for  $K_s$ ,  $K_p$ , and  $k_{off2}$  to those reported in Table 3. The conclusion is that accounting for the expected complicating and retarding influences had little effect on the identification of the key kinetics of the enzymatic process.

The assertion, “All models are wrong but some are useful,” attributed to George E. P. Box [18] is appropriate for the models and analyses presented here. There are several different

paths for the metabolism of salicylates [19] with different intermediate enzymes with different  $V_{\max}$ 's and  $K_m$ 's [20]. If that weren't bad enough, taking plasma concentrations from multiple subjects and averaging them seems also somewhat dubious. Although we have been successful in fitting population averages from three different studies and demonstrating that using all the data markedly improves the apparent resolution in the parameter estimates, the results remains questionable. However, the critical message from this paper is that one cannot estimate the effective  $K_m$  from either the low dose or the high dose data alone. One gets an approximate estimate from mid dose data. Then by using simultaneously the high mid and low dose data one gets not only confirmation of the approximation provided by the mid dose data, but increased accuracy for that estimate, presuming of course, that these different groups of humans are essentially similar. The variance of the parameter estimates are actually small compared to getting  $K_m$ 's from general sources like KEGG, and do represent human *in vivo* conditions, so making the values particularly relevant to popular usage. Much narrower confidence ranges can be determined using isolated enzymes in test-tube experiments, e.g. as for xanthine oxidase [21] or for glycolysis [22] but the conditions are rather different from *in vivo*. There is no doubt that greater precision would be gained if we could fit detailed data from individual subjects, and account for individual characteristics such as dose per kilogram of body weight, sex of subject, age of subject, etc.; this would allow us to assess population variances meaningfully.

The analyses using B-H/M-M and the differential equations for the enzyme model both provided comparisons of the results of individual versus simultaneous analysis of the three data sets, (Tables 2 and 4) giving evidence that better estimates of parameters are obtained when the analysis is required to include all the data at once. This is virtually always the case, and is the reason for undertaking large scale, multiscale modeling of biological systems, namely to enable the systematic, simultaneous analysis of multiple data sets simultaneously on multiple components of the system. Experiments designed to provide many measures of concentrations, fluxes, conditions, temperatures, and variant perturbations of the system are important for serious modeling analyses to assess working hypotheses on a biological system.

Are the *a priori* conditions for considering the three sets of data together valid? A difficult question gives rise to an insecure answer: the groups were assayed by three different investigative teams at quite different times. But the measurement of plasma salicylate concentrations was pretty standardized by that time and reasonably accurate, well within the range of variation of the different people in each group. Probably sex differences should have been accounted for. But all were adult humans, making it reasonable to expect the variation in  $K_m$ 's to be small compared to the huge range among species found for most enzymes in the KEGG repository. None of even the high dose group critically ill, so that their general conditions were close to normal. Our presumption that the groups were similar cannot be proven, but it would be as difficult to prove that they were not. Doubt lingers, but our judgment is that combining data sets in the analysis is more useful than not.

Extending the analysis of multiple data sets to experiments where the relationships on the data are purely statistical, and are so inaccurate that only log2-fold comparisons are near the threshold for statistical evaluation, as in mRNA array data, is *not* compatible with our

approach. “The invalid assumption that correlation implies cause is probably among the two or three most serious and common errors of human reasoning.”. Stephen Jay Gould [23]. Array analyses, mRNA and protein, reveal statistical associations, not relationships, mechanisms or causation. The *a priori* condition for biophysically and biochemically-based physiological modeling analysis is that one must have firm knowledge of system connectivity and stoichiometry, which is to say cause and effect relationships amongst elements of the modeled system (the “hypothesis”). One cannot conceive, even from replicated experiments done under the same conditions providing large amounts of noisy array data, of gaining much confidence concerning the nature of associations among chemical constituents, and even less in the parameter values.

The models described here are available on the Physiome Model Repository as Model 369 at [www.physiome.org](http://www.physiome.org). They and model 377 can be run over the web or downloaded and run on one’s own computer under the modeling system JSim. JSim can also be downloaded from the same site.

## 7. CONCLUSIONS

The modeling analysis of data, whether it is to provide descriptors or to determine mechanisms by which a system functions, gains accuracy by fitting several sets of data simultaneously with a common set of parameters. The greater the variety of good information represented by a single model the better the estimates of model parameters and the more secure the position of the model as a reasonable working hypothesis. What one seeks in biological modeling is a combination of goals: a secure description from which to make classifications; a comprehensive understanding of a self consistent system; a physicochemical system consistent with the laws of nature; an evaluation of confidence ranges for parameters and for the behavior of the system’s variables. In this study we use literature data covering a wide range of salicylate concentrations to estimate the parameters governing the clearance from the body, particularly on its enzymatic degradation. The range of the data, covering three-hundred fold in concentrations in three diverse groups, constrained the parameter estimates so that their coefficients of variation were less than 5%, a result not often achievable in clinical studies even with good experiment design, and emphasizing the power of integrating data from different sources.

## REFERENCES

1. Stone E. An account of the success of the bark of the willow in the cure of agues. In a letter to the right honourable george earl of macclesfield, president of R. S. from the Rev. Mr. Edmund Stone of Chipping-Norton in Oxfordshire. Philosophical Transactions of the Royal Society (1683–1775). 53:195–200. 1763.
2. Forman WB, Davidson ED, Webster LT Jr. Enzymatic Conversion of Salicylate to Salicylurate. Mol. Pharmacol. 1971; 7:247–259. [PubMed: 5571642]
3. Levy G. Pharmacokinetics of salicylate elimination in man. J. Pharm. Sci. 1965; 54:959–967. [PubMed: 5862532]
4. Levy G. Clinical pharmacokinetics of salicylates: A re-assessment. British J. of Pharmacology. 1980; 10(S2):285–290.

5. Knights, KM.; Miners, JO. Encyclopedia of drug metabolism and interactions. Vol. 6. John Wiley and Sons, Inc.; 2012. Amino acid conjugation: A novel route of xenobiotic carboxylic acid metabolism in man; p. 18
6. Grootveld M, Halliwell B. 2, 3-Dihydroxybenzoic acid is a product of human aspirin metabolism. *Biochemical Pharmacology*. 1988; 37(2):271–280. [PubMed: 3342084]
7. Benedek IH, Joshi AS, Pieniaszek HJ, SY King SY, Kornhauser DM. Variability in the pharmacokinetics and pharmacodynamics of low dose aspirin in healthy male volunteers. *J. Clin. Pharmacol.* 1995; 35:1181–1186. [PubMed: 8750369]
8. Aarons L, Hopkins K, Rowland M, Brossel S, Thiercelin JF. Route of administration and sex differences in the pharmacokinetics of aspirin, administered as its lysine salt. *Pharmaceutical Res.* 1989; 6:660–666.
9. Prescott LF, Balali-Mood M, Critchley JA, Johnstone AF, Proudfoot AT. Diuresis or urinary alkalisation for salicylate poisoning? *Br Med J (Clin Res Ed)*. 1982; 285(6352):1383–1386.
10. Butterworth E, Raymond GM, Jardine B, Neal ML, Bassingthwaighte JB. JSim, an open-source modeling system for data analysis [v3]. *F1000 Research*. 2014; 2(288):19.
11. Chizeck HJ, Butterworth E, Bassingthwaighte JB. Error detection and unit conversion. Automated unit balancing in modeling interface systems. *IEEE Eng Med Biol.* 2009; 28(3):50–58.
12. Michaelis L, Menten ML. The kinetics of invertase action. *Biochem. Z.* 1913; 49:333–369.
13. Briggs GE, Haldane JBS. A Note on the Kinetics of Enzyme action. *Biochem. J.* 1925; 19:338–339. [PubMed: 16743508]
14. Ho PC, Triggs EJ, Bourne WA, Heazlewood VJ. The effects of age and sex on the disposition of acetylsalicylic acid and its metabolites. *Br. J. Clin. Pharmac.* 1985; 19:675–684.
15. Bassingthwaighte JB, Butterworth E, Jardine B, Raymond G. Reifeld, Brad; Mayeno, Arthur N. Compartmental modeling in the analysis of biological systems. "computational toxicology. 2012; 1(929):391–438. *Methods in Molecular Biology*.
16. Hofmeyr J-HS, Cornish-Bowden A. The reversible Hill equation: How to incorporate cooperative enzymes into metabolic models. *Comput Appl Biosci.* 1997; 13:377–385. [PubMed: 9283752]
17. Bloch R, Sweeney G, Ahmed K, Dickinson C, Ingram D. MacDOPE: A simulation of drug disposition in the human body: Applications in clinical pharmacokinetics. *Br J Clin Pharmacol.* 1980; 10:591–602. [PubMed: 7470372]
18. Box GEP. Science and statistics. *J. Am. Stat. Assoc.* 1976; 71:791–799.
19. Hutt AJ, Caldwell L, Smith RL. The metabolism of aspirin in man: A population study. *Xenobiotica.* 1986; 16:239–249. [PubMed: 3705620]
20. Kuehl GE, Bigler J, Potter JD, Lampe JW. Glucuronidation of the aspirin metabolite salicylic acid by expressed UDP-glucuronosyltransferases and human liver microsomes. *Drug Metab Dispo.* 2006; 34(2):199–202.
21. Bassingthwaighte JB, Chinn TM. Reexamining Michaelis-Menten enzyme kinetics for xanthine oxidase. *Adv Physiol Educ.* 2013; 37:37–48. [PubMed: 23471247]
22. Lambeth MJ, Kushmerick MJ. A computational model for glycogenolysis in skeletal muscle. *Ann Biomed Eng.* 2002; 30:808–827. [PubMed: 12220081]
23. Gould, SJ. *The Mismeasure of Man*. New York: W. W. Norton; 1996. p. 272 ISBN: 0-393-03972-2



## APPENDIX

### Appendix 1. A: First order decay model

```

import nsrunit; unit conversion on;
math Decay {
// INDEPENDENT VARIABLE
realDomain t hour; t.min=0; t.max=16.0; t.delta=0.05;
// PARAMETERS: L for Low dose, M for Medium dose, and H for High dose
real LSO = 4.61 mg/L, MS0 = 71.8 mg/L, HS0 = 338 mg/L; // Initial concentration at t=0
real Lk = 0.33 1/hour, Mk = 0.156 1/hour, Hk = 0.0002 1/hour; // decay rates
// DEPENDENT VARIABLES
real LS(t) mg/L, MS(t) mg/L, HS(t) mg/L; // Model concentrations for 3 data sets
// INITIAL CONDITIONS
when(t=L.min) {LS=LS0; MS=MS0; HS=HS0;} //Concentrations projected back to t = 0
// ORDINARY DIFFERENTIAL EQUATIONS
LS.t = - Lk*LS; // rate of disappearance of S in the low dose case
MS.t = - Mk*MS; // rate of disappearance of S in the medium dose case
HS.t = - Hk*HS; // rate of disappearance of S in the high dose case
} // program end

```

### Appendix 2. Model II: B-H/M-M model

```

import nsrunit; unit conversion on;
import nsrunit; unit conversion on;
math BH_MM { // B-H and Michaelis-Menten use same equation but differing assumptions

realDomain t hour; t.min=0; t.max=16.0; t.delta=0.05; // defining time domain

real LSO = 4.6 mg/L, MS0 = 66 mg/L, HS0=337 mg/L; // Init conc at t=0 defined
real LBH(t) mg/L, MBH(t) mg/L, HBH(t) mg/L; //defining variables, concentration-time
curves
when (t = t.min) {LBH = LSO; MBH = MS0; HBH = HS0;} //initial conditions applied
real Km = 29.96 mg/L; // arbitrary starting value
real Vmax = 7.7 mg/(L*hour); // arbitrary starting value
real VmaxOverKm = Vmax/Km; // equivalent first order reaction rate, applicable at low concn

LBH.t = - Vmax*LBH / (Km + LBH); // LBH to be fitted to the low dose data
MBH.t = - Vmax*MBH / (Km + MBH); // MBH to be fitted to the medium dose data
HBH.t = - Vmax*HBH / (Km + HBH); // HBH to be fitted to the high dose data

realDomain S mg/L; S.min=1e-1; S.max=1e3; S.delta=1e-1; //defining a concentration domain, S
real dSdt(S) mg/(L*hour); //defining a flux on this domain
dSdt = - Vmax*S/(Km+S); // equation for M-M flux as fn of S

} // program end

```

### Appendix 3. Model III: Enzyme model

```

import nsrunit; unit conversion on;
math Enzyme { /* Three identical models used to weight the three data
                sets individually for optimization.
                L is low dose, M is mid dose, H is high dose,
                S: salicylic acid, E: free enzyme, SE: the complex, P: product */
// The /* and */ mark the start and end of a section not to be compiled
// INDEPENDENT VARIABLE
realDomain t hour; t.min=0; t.max=90.0; t.delta=0.1;
// PARAMETERS FOR THE THREE MODELS ANALYZING THREE DATA SETS

real kon1 = 3    L*mg(-1)*sec(-1), // On rate for SA + E → SE
koff1      1/sec, // Off rate for SE -> SA + E
kon2       L/(mg*sec), // On rate for P + E -> SE
koff2      = 13  1/sec, // Off rate for PE -> P + E
Etot       = 1.5e-4 mg/L, // Total enzyme (Coenzyme A)
Km         mg/L, // Km = (koff1+koff2)/kon1, Michaelis const
Vmax       mg/(L*hr), // Vmax = koff2*Etot
Ks         = 10  mg/L, // = koff1/kon1, dissociation const for S binding to E
Kp         = 100 mg/L; // = koff2/kon2, dissociation const for P binding to E
// CALCULATED PARAMETERS
koff1      = kon1*Ks; // solving for koff1
Kp         = koff2/kon2; // solving for kon2
Vmax       = koff2*Etot; // reaction velocity at enzyme saturation
Km         = (koff1+koff2)/kon1; // Michaelis const. (approx = Ks when koff2 is small)

// INITIAL DOSE PARAMETERS, PREFIXED L, M, H, FOR LOW, MID, AND HIGH DOSES
real LS0 = 5.07 mg/L,
MS0 = 64.59 mg/L,
HS0 = 335.0 mg/L,
// define MODEL VARIABLES as fns of time: Substrate, complex, enzyme, product
LS(t) mg/L, LSE(t) mg/L, LE(t) mg/L, LP(t) mg/L, // Low Conc study
MS(t) mg/L, MSE(t) mg/L, ME(t) mg/L, MP(t) mg/L, // Mid Conc study
HS(t) mg/L, HSE(t) mg/L, HE(t) mg/L, HP(t) mg/L, // High Conc study
// INITIAL CONDITIONS:
when(t=t.min) {LS = LS0; LSE = 0; LP=0;
MS = MS0; MSE = 0; MP=0;
HS = HS0; HSE = 0; HP=0; }

// ORDINARY DIFFERENTIAL AND MASS BALANCE EQUATIONS
LS:t = -kon1*LS*LE + koff1*LSE;
LSE:t = kon1*LS*LE - koff1*LSE - koff2*LSE + kon2*LE*LP;

```

```
LP:t =          koff2*LSE - kon2*LE*LP;
LE   =  Etot - LSE;

MS:t = -kon1*MS*ME + koff1*MSE;
MSE:t = kon1*MS*ME - koff1*MSE - koff2*MSE + kon2*ME*MP;
MP:t =          koff2*MSE - kon2*ME*MP;
ME   =  Etot - MSE;

HS:t = -kon1*HS*HE + koff1*HSE;
HSE:t = kon1*HS*HE - koff1*HSE - koff2*HSE + kon2*HE*HP;
HP:t =          koff2*HSE - kon2*HE*HP;
HE   =  Etot - HSE;
} program end
```

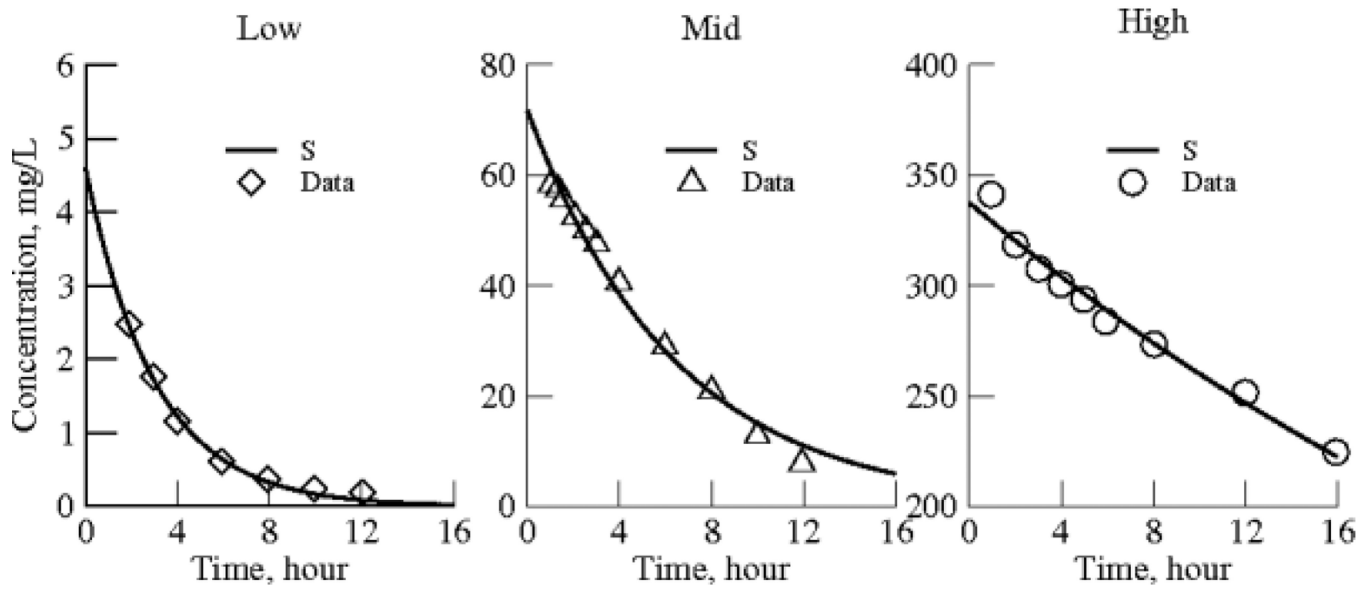


**Fig. 1. Salicylate decay curves for low, medium and high doses from three separate studies**  
Each is a group-averaged set of data from humans; Left panel: Benedek95; middle panel: Aarons89; right panel: Prescott82. Each data set is fitted with Model 1, single exponential functions with the half-life and an initial value of concentration for each dose group as the sole parameters. Parameter values and standard deviations for the model solutions to Eq 2 are given in Table 1

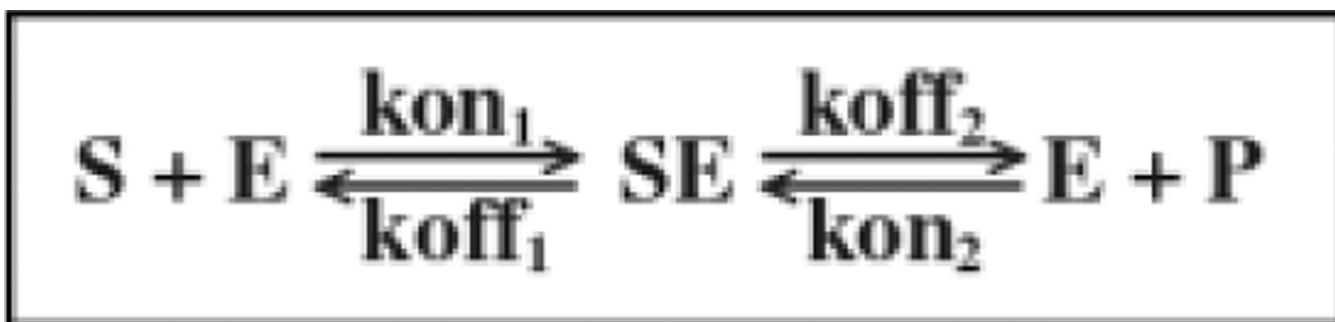


**Fig. 2. Reversible enzymatic reaction**

Substrate salicylate, S, combining with free enzyme, E, to form complex, SE, reacts to form product, P, and release free enzyme, E, to react with another substrate molecule

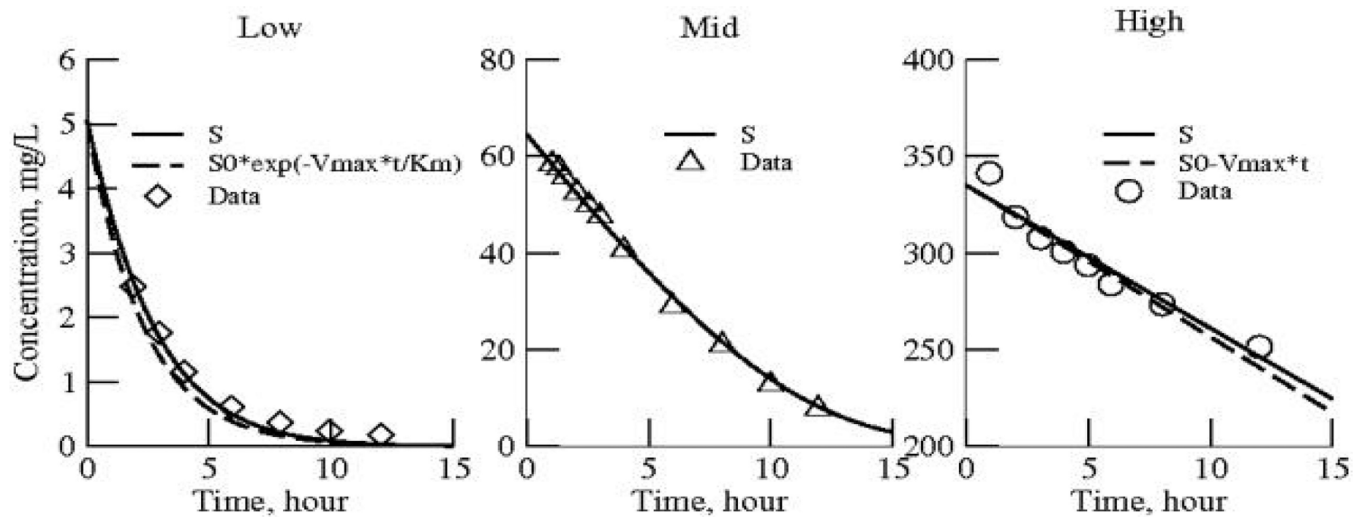


**Fig. 3. Fitting the Briggs-Haldane / Michaelis-Menten model (solid lines) to the three data sets simultaneously**

The five parameters are in Table 2, right column. For comparison, the dashed curve for the low dose panel represents the first order solution to the BH-MM equation, the rate constant at low concentrations being  $V_{\max} / K_m$ . The dashed line in the high dose panel is the zero order solution to the BH-MM equation, at the rate  $V_{\max}$ . The estimate of the  $K_m$ , 18.2 mg/L, is more than any of the concentrations of the low dose data but less than any of those of the high dose data, meaning that its strongest influence comes from the mid dose data

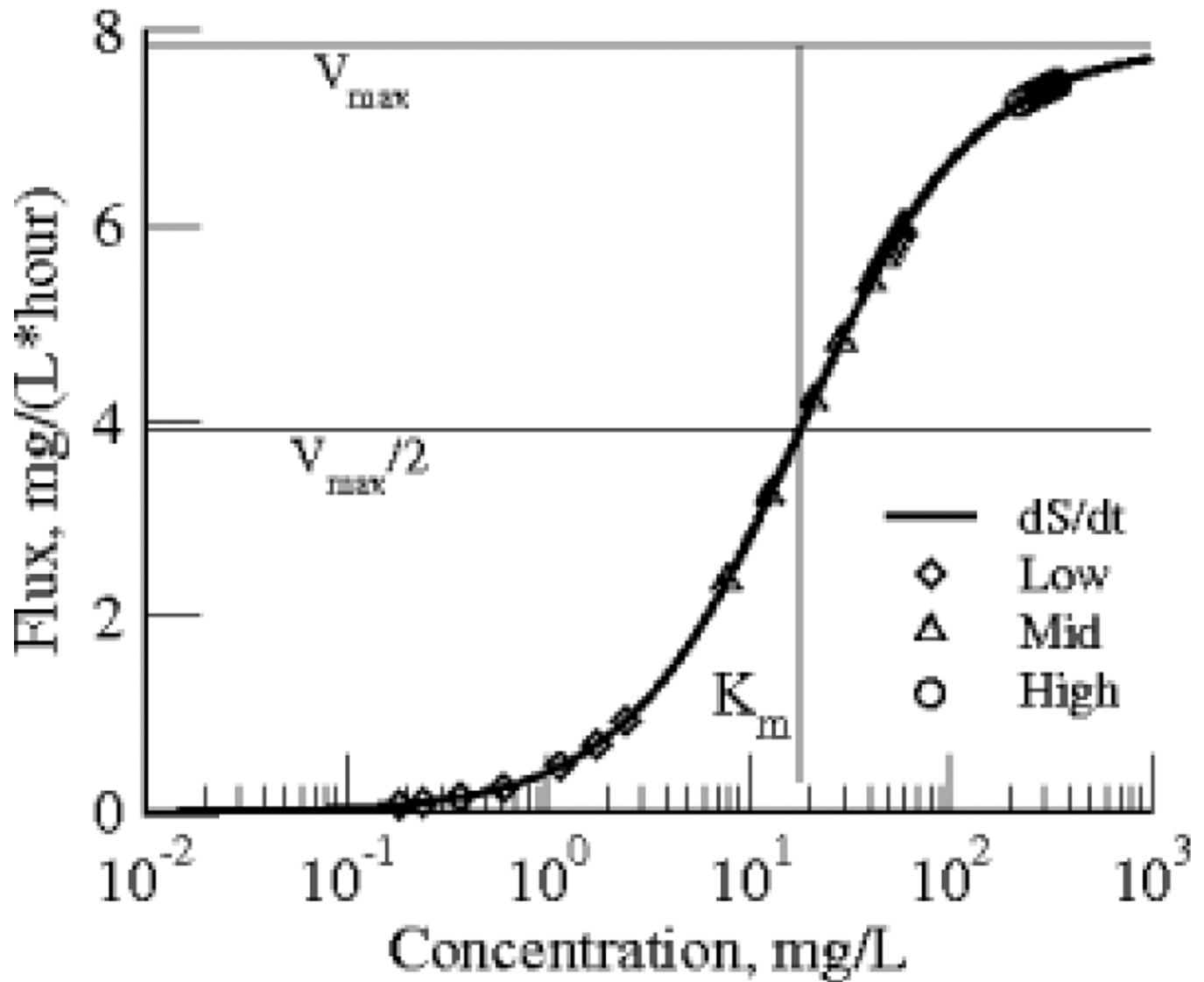


**Fig. 4. Clearance of S,  $dS/dt$ , versus S, the traditional Michaelis -Menten plot, describes the best fit of the model solution to all three data sets**

At  $V_{max}/2$  the concentration  $S = K_m$ . The intersection is at  $K_m = 18.2$  mg/L,  $V_{max}/2 = 3.9$  mg/(L\*hour). The abscissa indicates the low dose data (diamonds), mid dose (triangles), and high dose (circles) mapping to the fluxes on the ordinate, just as the  $K_m$  maps to  $V_{max}/2$

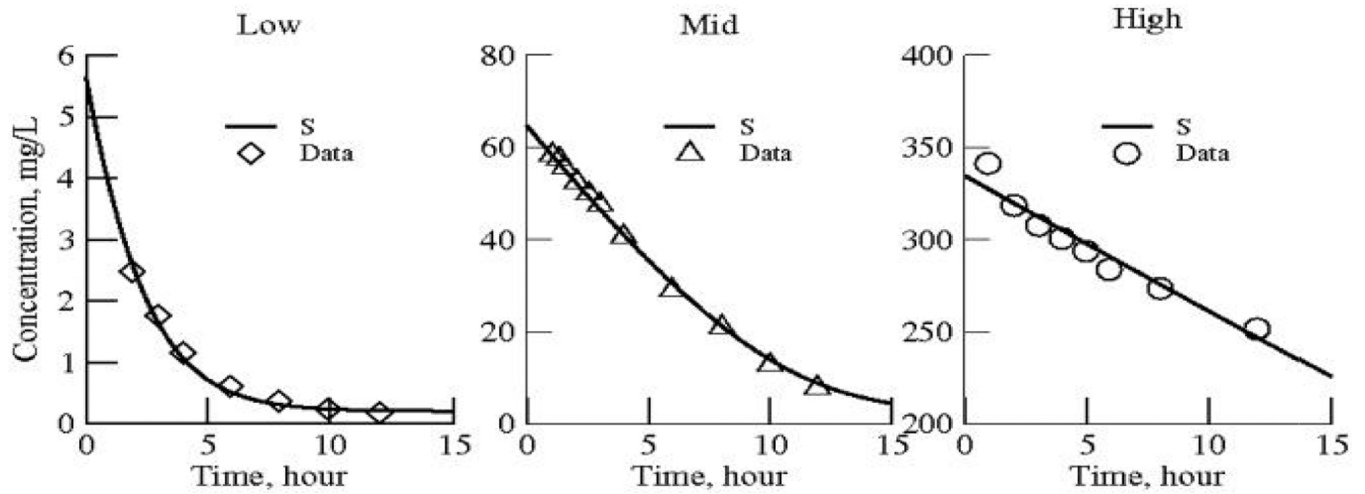


**Fig. 5. Fitting of the enzyme model solution for  $S(t)$  (heavy line in each plot) using simultaneous optimization to fit all three data sets**

The fitting parameters are given in Table 3, right 3 columns. The parameter values do not differ significantly between using 3 free parameters ( $K_s$ ,  $K_p$ , and  $k_{off2}$ ) and using 6 free (those + the 3 initial concentrations), but the estimated confidence ranges do differ, the degrees of freedom being reduced by fixing the values of the three initial concentrations, removing them from the estimation procedure



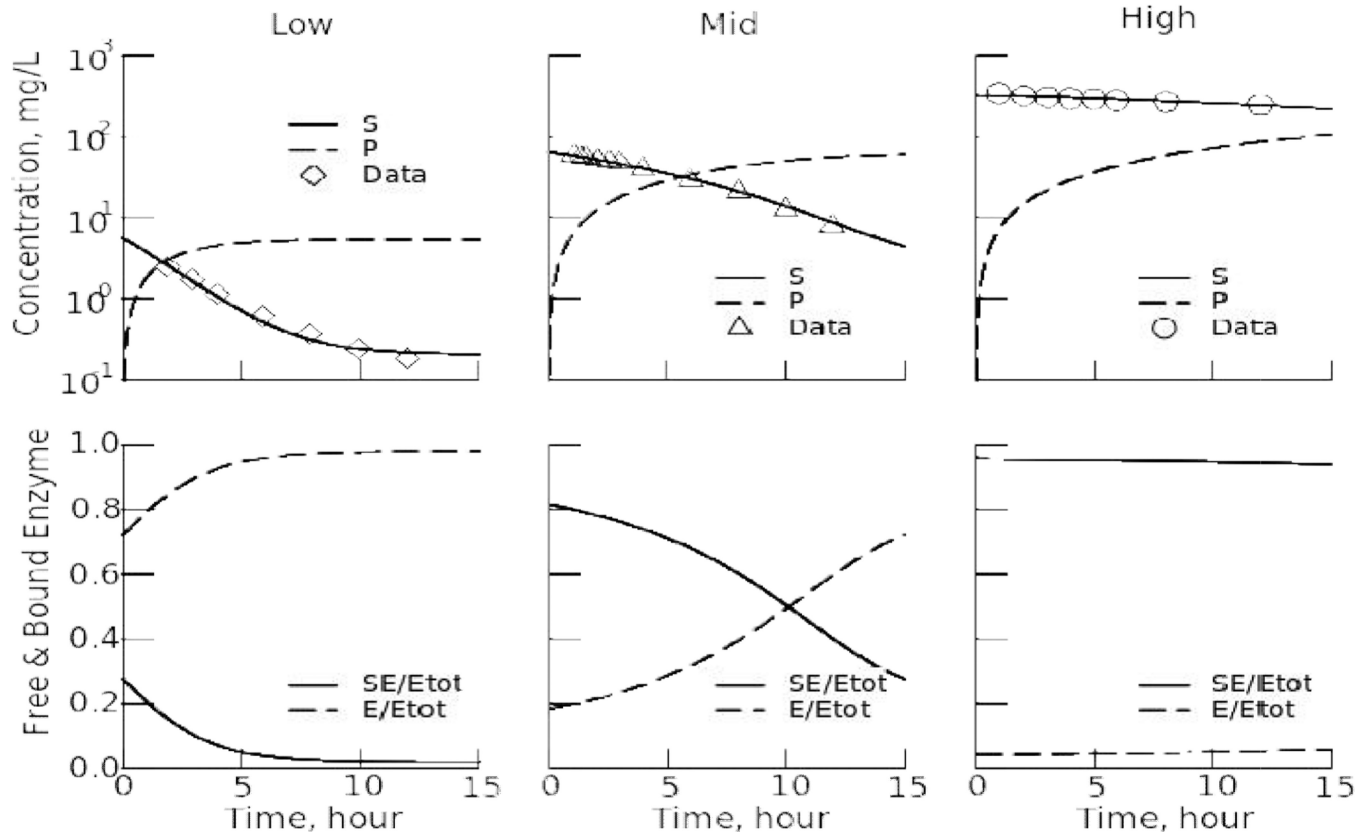


**Fig. 6. Model fitting to the three data sets simultaneously: (Parameters are in Table 3 right column)**

Top Panels: Data and model fits on a semilog plot, fitting S and predicting P. Lower panels: The fractional enzyme occupancy,  $SE/E_{tot}$  and free unbound enzyme E versus time, for the same three data sets as shown in the top panels. For the low dose data the enzyme is mostly free, i.e.  $SE/E_{tot}$  is low; for the high dose data, there is very little free

**Table 1**  
**Exponential decay model: Optimized parameters**

| Parameter value<br>$\pm 1$ SD* | Initial concn<br>$S_0$ , mg/L | Decay rate constant,<br>fraction/hr k, hr <sup>-1</sup> | Half-life, min | RMS/ $S_0$ |
|--------------------------------|-------------------------------|---|----------------|------------|
| Low concn                      | 4.61 $\pm$ 0.74               | 0.332 $\pm$ 0.016                                       | 126 $\pm$ 7    | 0.015      |
| Middle concn                   | 71.8 $\pm$ 1.75               | 0.156 $\pm$ 0.008                                       | 267 $\pm$ 14   | 0.026      |
| High concn                     | 337.5 $\pm$ 10.3              | 0.026 $\pm$ 0.002                                       | 1600 $\pm$ 100 | 0.015      |

Optimized values for initial concentrations and rates of decay using the first order clearance model. The standard deviations of the estimates came from optimizing the group data sets individually

Author Manuscript

Author Manuscript

Author Manuscript

Author Manuscript

**Table 2**  
**Model 2: B-H/M-M: Parameters from optimizations**

Values from optimizing Briggs-Haldane/Michaelis-Menten model.

| Parameter<br>±1 SD            | Low dose<br>individual optim | Mid dose<br>individual optim | High dose<br>individual optim | Simultaneous<br>optimization |
|-------------------------------|------------------------------|------------------------------|-------------------------------|------------------------------|
| $K_m$ mg/L                    | Fixed at 24.1                | 24.1±5.4                     | Fixed at 24.1                 | 18.2±2.6                     |
| $V_{max}$ mg/(L*hr)           | 8.4±0.49                     | 9.2±0.89                     | 7.7±0.56                      | 7.85±0.38                    |
| $V_{max} / K_m$ 1/hr          | 0.35±0.021                   | 0.40±0.12                    | 0.36±0.011                    | 0.44±0.07                    |
| $LS_0$ mg/L                   | 5.07±0.23                    | -                            | -                             | 5.07±0.48                    |
| $MS_0$ mg/L                   | -                            | 65.99±0.57                   | -                             | 64.59±0.99                   |
| $HS_0$ mg/L                   | -                            | -                            | 333.1±1.6                     | 335.0±2.5                    |
| Wgt in Simult<br>Optimization | 1.6435                       | 0.0211                       | 0.0034                        | Curve Wgts at left           |
| $\Sigma S'_i - S_i /S'_i/N_p$ | 0.170                        | 0.014                        | 0.017                         | 0.096                        |

The shaded regions mark estimates of parameters with such low sensitivities that the results had no meaning until we decided to use the estimate of  $K_M$  from the mid dose data as fixed values of  $K_M$  and optimized on that basis. If the calculations for the shaded boxes were chosen in accord with the  $K_M$  from the simultaneous fit (right column) the  $V_{max}$  would change in proportion and  $V_{max} / K_M$  would not change. The SD for  $V_{max} / K_M$  for simultaneous optimization was calculated by a Monte Carlo iterative optimization using the MML function for setting the five parameters ( $V_{max}$ ,  $K_M$ , and the three  $S_0$ 's) defined by their individual Gaussian probability density functions, doing  $10^4$  optimizations. The SD for  $V_{max}/K_M$  for the mid dose data was found by using Caladis ([www.Caladis.org/compute/](http://www.Caladis.org/compute/)), also a Monte Carlo method. Error assessments are provided in the bottom row, the fractional error per point,  $\Sigma|S'_i - S_i|/S'_i/N_p$

**Table 3**  
**Enzyme kinetic model: Estimated parameters under three conditions**

Estimated parameter values for the enzyme model

| Parameter   | A. Optimizing to fit individual data sets at each dose level |                           |                         | B. Simultaneous optimization to fit all three dose level data using 6 free parameters |                        |             | C. Simultaneous optimization to fit all three dose levels with $S_0$ fixed |                        |             |
|---|--|---------------------------|-------------------------|---|------------------------|-------------|--|------------------------|-------------|
|   | Low dose<br>$\pm 1$ SD                                       | Medium<br>dose $\pm 1$ SD | High dose<br>$\pm 1$ SD | How<br>obtained   | Estimate<br>$\pm 1$ SD | SD/<br>Mean | How<br>obtained  | Estimate<br>$\pm 1$ SD | SD/<br>Mean |
| $K_S$ mg/L  | 6.33 $\pm$ 2.10  | 8.30 $\pm$ 2.54           | 181 $\pm$ 131           | Opt   | 11.9 $\pm$ 0.66        | $\pm$ 5.5%  | Opt  | 10.44 $\pm$ 0.18       | $\pm$ 1.7%  |
| $K_P$ mg/L  | 169 $\pm$ 67   | 246 $\pm$ 130             | 91 $\pm$ 68             | Opt   | 335 $\pm$ 30.4         | $\pm$ 9.1%  | Opt  | 273.5 $\pm$ 6.5        | $\pm$ 2.4%  |
| $k_{off2}$ 1/sec  | 7.45 $\pm$ 1.96  | 14.7 $\pm$ 0.67           | 55.4 $\pm$ 30.4         | Opt   | 15.4 $\pm$ 0.29        | $\pm$ 1.9%  | Opt  | 14.82 $\pm$ 0.13       | $\pm$ 0.9%  |
| $LS_0$ mg/L   | 4.57 $\pm$ 0.12  | --                        | --                      | Opt   | 5.39 $\pm$ 0.09        | $\pm$ 1.7%  | Fixed  | 5.67                   | --          |
| $MS_0$ mg/L   | --   | 65.8 $\pm$ 0.25           | --                      | Opt   | 65.5 $\pm$ 0.22        | $\pm$ 0.3%  | Fixed  | 64.9                   | --          |
| $HS_0$ mg/L   | --   | --                        | 353 $\pm$ 6.0           | Opt   | 336 $\pm$ 0.98         | $\pm$ 0.3%  | Fixed  | 335                    | --          |
| $k_{on1}$ L/(mg $\cdot$ sec)                                | 3.0  | 3.0                       | 3.0                     | Fixed   | 3.0                    | --          | Fixed  | 3                      | --          |
| $F_{TOT}$ mg/L  | 1.5e-4   | 1.5e-4                    | 1.5e-4                  | Fixed   | 1.5e-4                 | --          | Fixed  | 1.5e-4                 | --          |
| $K_m$ mg/L  | 8.82 $\pm$ 2.75  | 13.2 $\pm$ 2.76           | 199 $\pm$ 131           | Calc  | 17.1 $\pm$ 0.75        | $\pm$ 4.4%  | Calc   | 15.4 $\pm$ 0.22        | $\pm$ 1.4%  |
| $V_{max}$ mg/(L $\cdot$ hr)<br>= $K_S + k_{off2} / k_{on1}$ | 4.02 $\pm$ 1.06  | 7.94 $\pm$ 0.36           | 29.9 $\pm$ 16.4         | Calc  | 8.30 $\pm$ 0.15        | $\pm$ 1.9%  | Calc   | 8.00 $\pm$ 0.07        | $\pm$ 0.9%  |
| $k_{off1}$ 1/sec = $K_S \cdot k_{on1}$                      | 19.0 $\pm$ 6.3   | 24.9 $\pm$ 7.6            | 542 $\pm$ 393           | Calc  | 35.8 $\pm$ 1.99        | $\pm$ 5.5%  | Calc   | 31.3 $\pm$ 0.55        | $\pm$ 1.7%  |
| $k_{on2}$ L/(mg $\cdot$ sec)<br>= $k_{off2} / K_P$          | 0.0467 $\pm$ 0.0064  | 0.077 $\pm$ 0.044         | 6.4 $\pm$ 20.5          | Calc  | 0.046 $\pm$ 0.0042     | $\pm$ 9.2   | Calc   | 0.054 $\pm$ 0.0014     | $\pm$ 2.5%  |

Assuming a fixed value for  $k_{on1} = 3$  L/(mg $\cdot$ sec), we used three approaches: [A] (columns 2 to 4): "Unconstrained" fitting of the three data sets individually; [B] (Columns 5 to 7): Simultaneous fitting of the three data sets using  $K_S$ ,  $K_P$ , and  $k_{off2}$ , and the three initial values,  $S(=0)$ ; [C] (Columns 8 to 10): Simultaneous fitting of the three data sets using only  $K_S$ ,  $K_P$ , and  $k_{off2}$ , with all other parameters fixed. The resulting fit is displayed in Fig. 5